Sheared magnetospheric plasma flows and discrete auroral arcs: a quasi-static coupling model

M. M. Echim, M. Roth, J. de Keyser

Ann. Geophys., 25, 317–330, 2007
www.ann-geophys.net/25/317/2007/

Annales Geophysicae

Sheared magnetospheric plasma flows and discrete auroral arcs: a quasi-static coupling model

M. M. Echim[1,*], **M. Roth**[1], **and J. De Keyser**[1]

[1]BIRA-IASB, Avenue Circulaire 3, 1180 Bruxelles, Belgium
[*]also at: the Institute for Space Sciences, Atomiştilor 409, 077125 Măgurele, Romania

Received: 13 November 2006 – Accepted: 22 January 2007 – Published: 1 February 2007

Abstract. We consider sheared flows in magnetospheric boundary layers of tangential discontinuity type, forming a structure that is embedded in a large-scale convergent perpendicular electric field. We construct a kinetic model that couples the magnetospheric structure with the topside ionosphere. The contribution of magnetospheric electrons and ionospheric electrons and ions is taken into account into the current-voltage relationship derived for an electric potential monotonically decreasing with the altitude. The solution of the current continuity equation gives the distribution of the ionospheric potential consistent with the given magnetospheric electric potential. The model shows that a sheared magnetospheric flow generates current sheets corresponding to upward field-aligned currents, field-aligned potential drops and narrow bands of precipitating energy, as in discrete auroral arcs. Higher velocity magnetospheric sheared flows have the tendency to produce brighter and slightly broader arcs. An increase in arc luminosity is also associated with enhancements of magnetospheric plasma density, in which case the structures are narrower. Finally, the model predicts that an increase of the electron temperature of the magnetospheric flowing plasma corresponds to slightly wider arcs but does not modify their luminosity.

Keywords. Magnetospheric physics (Auroral phenomena; Current systems; Magnetosphere-ionosphere interactions)

1 Introduction

Auroras reflect complex phenomena linking the solar wind, the magnetosphere and the upper atmosphere. These complicated links are often compared to a television set, where the solar wind is the source of electricity and the auroral oval reflects the vivid images drawn on the TV screen (the upper atmosphere) by field-aligned accelerated electrons emitted by an electron gun located in the magnetosphere. This whole complex system is responsible for some of the most spectacular events: discrete auroral arcs. They are dynamic and challenging auroral phenomena still not completely understood. In this paper we develop a quantitative model that describes the quasi-static coupling between sheared plasma flows in the magnetosphere and the activation of discrete auroral arcs. The model provides ionospheric parameters, like the latitudinal distribution of the electric potential, net parallel current, density and flux of precipitating energy as a function of plasma variables in the magnetosphere, like density, temperature and bulk velocity.

In this study we consider that the magnetospheric plasma bulk velocity has a gradient, or shear, in the direction perpendicular to a plasma interface of tangential discontinuity (TD) type, i.e., in a direction perpendicular to the magnetic field. We consider a simplified geometry consisting of a plane TD parallel to the yz plane; the magnetic field is everywhere parallel to the z-axis and the plasma bulk velocity is aligned with the y-axis. Plasma variables and field vary with x, the coordinate normal to the TD surface. A diagram that illustrates the magnetospheric sheared flow is given in Fig. 1a.

In-situ investigation provides observations of this type of flow in the terrestrial magnetosphere. We distinguish two types of configurations of sheared plasma flows in the Earth's magnetosphere.

(I) Sheared plasma flows were detected by satellites inside the Low Latitude Boundary Layer (LLBL) proper and/or at its interface with the plasma sheet or lobes (e.g. Lundin and Evans, 1985; Phan et al., 1997; Vaisberg et al., 2001). The total variation of the bulk velocity across the layer is limited for this class of events by the solar wind convection velocity. Lundin and Evans (1985) made correlations between satellite observations of plasma structures injected in the LLBL and the occurrence of high latitude, early afternoon, discrete auroral arcs. Roth et al. (1993) demonstrated from a theoretical

Correspondence to: M. M. Echim
(marius.echim@oma.be)

Published by Copernicus GmbH on behalf of the European Geosciences Union.

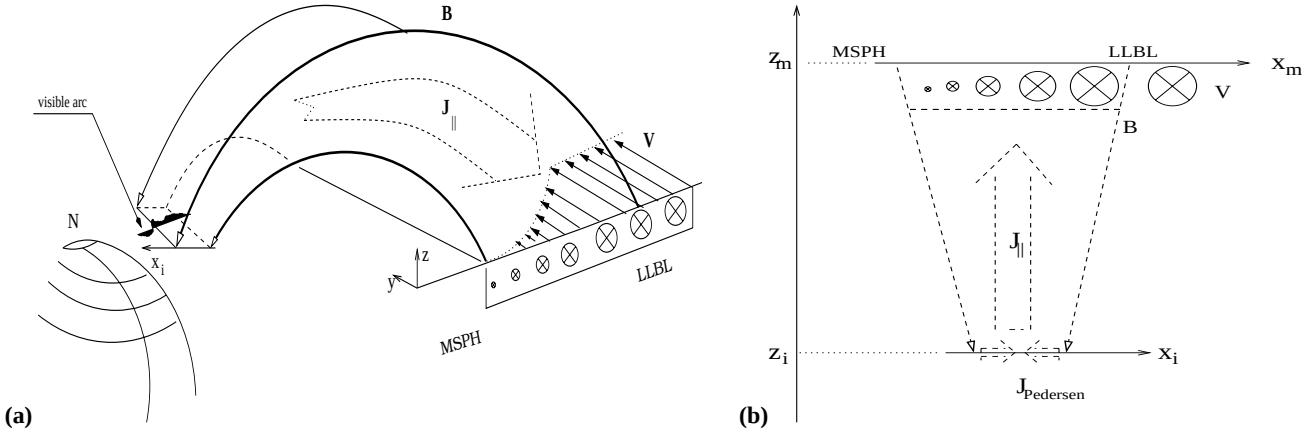

Fig. 1. Diagram illustrating the coupling between the magnetospheric sheared flow and the ionosphere. **(a)** A schematic 3-D view of the dusk flank; **(b)** A simpler, conical geometry has been adopted to describe a flux tube extended from lower/ionospheric altitudes (z_i) to upper/magnetospheric level (z_m). The upper boundary of the flux tube coincides with a magnetospheric sector that includes the sheared flow layer at the interface between the LLBL and Earthward region; the latter is labelled MSPH. The shear flow layer is described by a TD and plays the role of an auroral generator, as explained in the text. The velocity profile is illustrated by circles whose radius is proportional to the local value of the bulk velocity; the velocity is oriented anti-sunward, along the y-axis, into the page plane; the magnetic field lines and the parallel and horizontal currents are also illustrated.

kinetic point of view that the tangential discontinuities (TD) formed at the interface between plasmas with different temperatures and/or densities can be the site of an electromotive force. They argued that such TDs can play the role of generator for discrete auroral arcs, but did not investigate the effects of sheared flows.

(II) The Plasma Sheet and its boundary layers as well as the magnetotail are sites where high speed plasma flows and bursty bulk flows were observed on a wide range of locations (e.g. Baumjohann et al., 1990; Angelopoulos et al.,1992; Cao et al.,2006). High speed ion beams were reported by Grigorenko et al. (2002) at smaller scales. The effects of magnetospheric sheared flows on the aurora are subject of recent theoretical and experimental investigation. Sergeev et al. (1999); Fairfield et al. (1999); Zesta et al. (2000); Nakamura et al. (2001) showed that auroral activations correlate well with this type of sheared plasma flows in the Earth's magnetosphere. De Keyser (1999) has demonstrated that the polarization electric field of a tangential discontinuity in the plasma sheet can explain the ion drifts observed at subauroral latitudes during substorms.

In this study we investigate magnetospheric plasma flows and fields that correspond to the first configuration described above, i.e. the plasma interface in the LLBL region. We describe the boundary layer formed between a fast moving plasma and the background plasma at the dusk sector of the LLBL. A diagram of the plasma flow and fields modeled in this paper is given in Fig. 1. The plasma velocity has a strong shear across a boundary layer that is described by a tangential discontinuity.

The geomagnetic field lines couple the region of magnetospheric sheared flow with the topside ionosphere. We develop a quasi-static model that computes the ionospheric electrodynamic parameters (electrostatic potential, field-aligned current density, flux of precipitating energy) corresponding to a magnetospheric generator similar to the one described by Roth et al. (1993) and De Keyser (1999), with an added velocity shear. The electromotive force of the generator is given by the polarization electric field of the TD formed between magnetospheric sheared flows. We do not discuss here the causes and/or the driver of these enhanced flows; their existence is plausible from experimental data.

In the next section we briefly describe the kinetic TD structure and explain why it can play the role of an auroral generator. We also discuss the ionospheric load and the coupling mechanism with the high altitude potential. In Sect. 3 we discuss the vertical distribution of the plasma and fields. In Sect. 4 the ionospheric electrodynamic variables are numerically computed as a function of the magnetospheric plasma parameters. We discuss the relevance of these results for the formation of discrete auroral arcs. The paper concludes with a summary.

2 Coupling of the high altitude sheared flows and the polar ionosphere

In this section we describe the two main components of the auroral current circuit: the magnetospheric generator and the ionospheric load. We also discuss the coupling mechanism in a steady-state situation. We consider a high-altitude,

relatively hot and tenuous magnetospheric plasma, with a shear of the bulk velocity, connected by the same magnetic flux tube to the colder and denser ionospheric plasma. The geometry of the problem is illustrated in Fig. 1b. The equilibrium solution for the system of the two constituent plasmas is computed for a steady-state situation.

2.1 An auroral generator

In the plane TD layer the plasma flow is tangential to the discontinuity surface and the magnetic field component normal to it is equal to zero. However, because of charge separation effects there is a unidirectional electric field, perpendicular to the TD interface. In kinetic models of TDs the internal structure is solved, i.e. the profile of variation between the two asymptotic states at the two sides of a TD can be computed self-consistently.

In the TD considered in this study, the magnetospheric (MSPH) plasma is at rest at the left hand side, where it has density $N_{\rm M}$ and temperature $T_{\rm M}$, typical for the plasma sheet (PS). At the right hand side the plasma is in motion with a velocity $\boldsymbol{V}$ (perpendicular to the B-field and in the positive direction of the y-axis) and has density $N_{\rm L}$ and temperature $T_{\rm L}$. It will be called the LLBL plasma since it has properties typical for the Low Latitude Boundary Layer. The typical values of MSPH and LLBL plasma parameters used in this study are given in Table 1. Inside the transition layer all the variables vary with x, the coordinate normal to the TD plane, as illustrated in Fig. 1b. The relative orientation of the plasma bulk velocity and magnetic field correspond to a magnetospheric plasma flow on the dusk-side flank of the magnetosphere. It is assumed that the plasma flow (and its coupling to the ionosphere) is quasi-static, i.e. the external driver sustains the flow shear over time scales longer than the typical time needed for an electron to travel between the magnetosphere and the ionosphere.

A complete description of the TD kinetic model is beyond the scope of this study and can be found in the paper of Roth et al. (1996). A discussion of the effect of flow shears on the TD equilibrium conditions for the terrestrial magnetopause can be found in De Keyser and Roth (1997a, b). Two-dimensional solutions have been published by Echim and Lemaire (2005). Let us briefly recall the main principles.

We consider a TD for which the magnetic field is everywhere perpendicular to the plasma bulk velocity, thus we choose a unidirectional magnetic field parallel to the z-axis. As the velocity is aligned with the y-direction the convection electric field is parallel to the x-axis. Thus the z-component of the velocity of a charged particle is a constant and we are therefore free to consider the motion of this particle to be in the (xy) plane. In this plane, a particle (of mass m^α and charge $Z^\alpha e$, with e the magnitude of the elementary charge) is characterized by two constants of motion: the total energy, $H=1/2m^\alpha v^2+Z^\alpha e\Phi$, and the y-component of the canonical momentum: $p_y=m^\alpha v_y+Z^\alpha ea$ with Φ the electric potential and a the single component of the magnetic vector potential (in the geometry of Fig. 1, $\boldsymbol{A}$ is a unidirectional vector along the y-axis).

Table 1. Asymptotic values of the number density, temperature, bulk velocity of electrons ("−") and protons ("+") used to obtain the TD solutions illustrated by Figs. 2–3. The values of the parameters $l^{\pm}_{M,L}$ of each considered species are also given; $l^{\pm}_{M,L}$ is a parameter of the VDF that controls the width of the TD layer, as shown in the Appendix.

	$n^-=n^+$ [cm^{-3}]	T^- [eV]	T^+ [eV]	V [km/s]	l^-	l^+
$x=-\infty$ (MSPH)	0.5	200	1000	0	20	5
$x=+\infty$ (LLBL)	5	10	100	190	20	5

In the steady-state Vlasov kinetic approach, any function $f(H, p_y)$ can be a velocity distribution function. In practice, steady-state solutions are constructed using piecewise Maxwellian VDFs (Roth et al., 1996) that satisfy the asymptotic conditions describing the geometry of the problem. The analytical expressions of the VDFs used in this study as well as of their first order moments, including the charge and current densities, are given as functions of (Φ, a) in the Appendix; the electric and magnetic fields and their corresponding potentials (Φ, a) are computed numerically from the Maxwell's equations. Reintroducing the computed potentials in the analytical moments of the VDFs gives a complete description of the transition layer. Since space plasmas are in general quasineutral, the Maxwell-Poisson's equation for the unknown electric potential can be replaced by the quasineutrality equation.

Figures 2 and 3 show the TD solutions obtained for the interface between a stagnant plasma and a plasma in motion having different velocities and densities. The asymptotic parameters of the two populations, typical for a MSPH/LLBL transition, are given in Table 1. Figure 2 shows the structure of the transition layer obtained for three different flow speeds at the right hand side when all the other parameters keep the constant values given in Table 1. Figure 3 indicates what happens when the density of the moving plasma at the right hand side is varied while the other parameters of Table 1 are constant. A key feature of the solution is the linearly increasing electric potential in the LLBL, that gives the electric field in this region (first panels in Figs. 2 and 3). As such, the boundary layer is an unloaded source of electromotive force. Another characteristic of the TD is the scaling of the transition layer with the asymptotic temperatures. It is possible to obtain broader or thinner transition layers as a function of the asymptotic plasma temperature and/or bulk velocity as discussed in the Appendix. As Fig. 3 shows the profile of

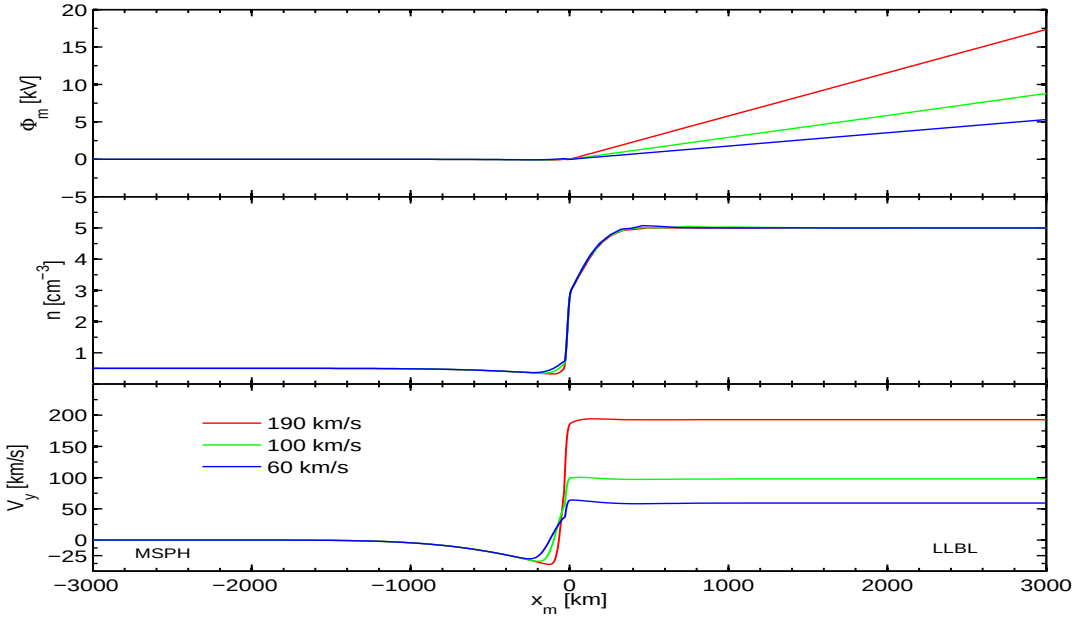

Fig. 2. Kinetic tangential discontinuity (TD) solution for the transition between magnetospheric (plasma sheet) plasma at rest (left hand side) and LLBL plasma moving in the y-direction (right hand side). The colors correspond to three different values of the plasma bulk speed $V{=}V_y$ ($V_x{=}V_z{=}0$ everywhere). The planar TD is centered at $x{=}0$, parallel to the yz plane. The panels show the variation with the x-coordinate (normal to the TD surface) of the magnetospheric electrostatic potential, Φ_m, number density, n and the plasma bulk velocity V.

the TD electric potential is not very sensitive to the plasma density in the LLBL.

In reality, however, this source of electromotive force is connected to the conducting ionosphere by the geomagnetic field lines, thus the current circuit is closed and the boundary layer plays the role of a generator in this circuit. When the TD generator is loaded, electric charges will be drained by field-aligned and dissipative ionospheric currents. Although the drainage of charges by field aligned currents may alter the TD profile, the electrostatic potential is maintained as long as the discharging currents are small enough and as long as the external driver sustains the gradient of the temperature and/or density and the shear of flow. Roth et al. (1993) have shown that for a TD formed at the interface of a magnetospheric plasma, with density of the order of $0.5\,\mathrm{cm}^{-3}$ and temperature of the order of 2.5 keV, coupled to the ionosphere, the time needed to alter significantly the TD structure is of the order of 1000 s. From this order of magnitude estimate one can argue that the TD generator can supply emf for sufficiently long intervals.

2.2 Horizontal Pedersen currents and coupling

An analysis of the magnetospheric generator based on the thermo-electric and gradient density effects at the interface between different plasma populations and the relationship of this generator to auroral arcs can be found in Roth et al. (1993). This paper gives a quantitative analysis of the ionospheric effects induced by a high altitude sheared flow across the TD. The electrostatic potential, density and temperature obtained from the kinetic description discussed above are used as input parameters for a quasi-static model of the magnetosphere-ionosphere coupling as described below.

In the ionosphere, where collisions are important, the ionospheric Hall and Pedersen electric conductivities take large values, in the plane normal to the magnetic field direction. Horizontal currents flow both in latitudinal and azimuthal directions. Lyons (1980, 1981) solved the one-dimensional current continuity equation that couples the field-aligned currents driven by a magnetospheric generator with the height-integrated horizontal ionospheric Pedersen current (I_p). Assuming that an auroral arc is aligned azimuthally and that the Hall current is neglected, the current continuity equation can be written as:

$$j_{||} = -\frac{dI_P}{dx_i} = \frac{d}{dx_i}\left(\Sigma_P \frac{d\Phi_i}{dx_i}\right) \tag{1}$$

In Eq. (1) the height-integrated Pedersen conductivity, Σ_P, can be a function of the flux of precipitating energy (Harel et al., 1977; Robinson et al.,1987) and implicitly of the potential drop, but here it is taken constant.

The ionospheric potential, Φ_i, has been computed by Lyons (1980) from the non-linear continuity differential equation (1) for an ad-hoc profile of Φ_m, the electrostatic

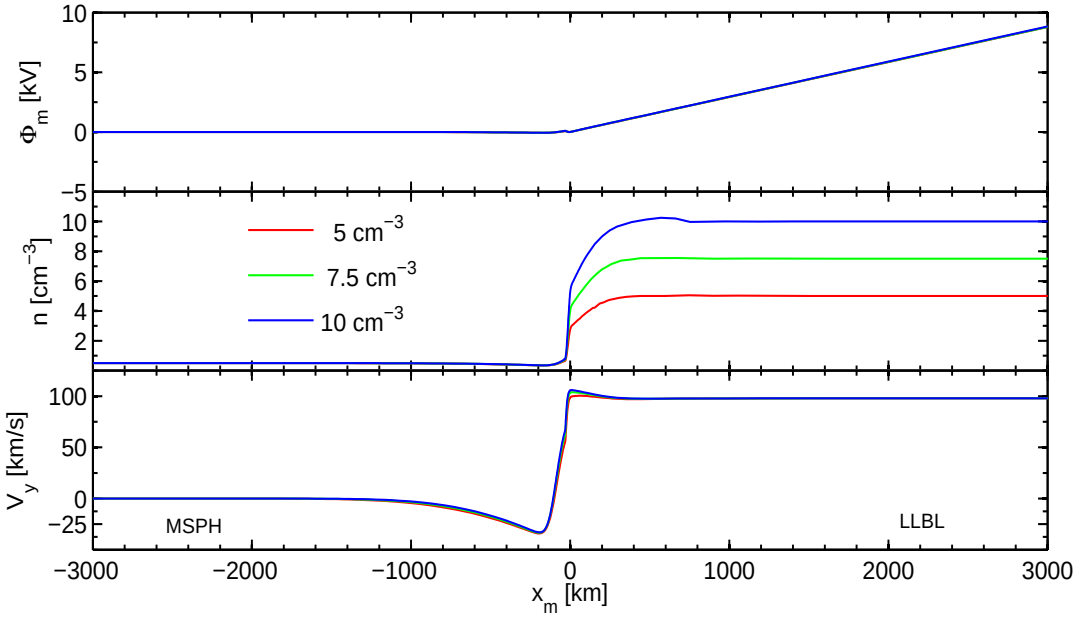

Fig. 3. Kinetic tangential discontinuity solution obtained for different values of the LLBL density (right side of the discontinuity); see caption of Fig. 2 for a description of the different panels.

potential in the magnetosphere. In Lyons' model, $\Phi_m(x_m)$ has been defined such that the resulting electric field is convergent, $\nabla \cdot \boldsymbol{E} < 0$. We will replace this ad-hoc solution by Φ_m computed from the TD model, which gives a potential profile with a fine structure embedded in a large-scale convergent electric field.

3 Vertical distribution of plasma and fields

Lyons' solution is obtained by taking into account only the precipitating magnetospheric electrons. The latter is the most important component when the field-aligned potential drop has significant values. In our model we add additional species as described below.

The variation with altitude of the velocity distribution function of the species that populate the same flux tube is derived from Liouville's theorem. A velocity distribution function that is a function of the constants of motion is a solution at each altitude (Lemaire and Scherer, 1971). Thus a Maxwellian VDF defined at ionospheric or magnetospheric altitude:

$$f_\nu^\alpha = N_\nu^\alpha \left(\frac{m^\alpha}{2\pi k T_\nu^\alpha} \right)^{\frac{3}{2}} e^{-\frac{H - Z^\alpha e Phi}{2kT_\nu^\alpha lpha}} \qquad (2)$$

is a solution of the stationary Vlasov equation at each altitude, z. In Eq. (2) the subscript ν identifies the ionospheric or magnetospheric origin of the different plasma species α, with temperature T_ν^α, mass m^α and charge $Z^\alpha e$. Such an exospheric-type kinetic solution is valid in phase space regions that vary with the local electric and magnetic potentials. Exospheric solutions have been successfully used to develop models of the polar wind with asymptotic VDFs that are Maxwellian (Lemaire and Scherer, 1971) or Kappa functions (Pierrard, 1996). The exospheric method has also been used to derive the parallel electric fields along auroral field lines (Knight, 1973; Lemaire and Scherer, 1973; Fridman and Lemaire, 1980).

When the variation of the potential with the altitude, $\Phi(z)$, is monotonic, the conservation of the total energy and of the magnetic moment completely determines the region of the phase space that is accessible for particles coming from both ends (Whipple, 1977). Thus the moments of the VDF can be computed as a function of the local electric potential and magnetic field and the parallel flux of particles is derived

Table 2. Reference density and temperature of the ionospheric species considered in the current-voltage relationship (Eqs. 5, 6). The charge densities were adjusted such that charge neutrality is satisfied.

	e^-	O^+	H^+
T[keV]	0.2	0.02	0.02
n[cm^{-3}]	7×10^3	6.5×10^3	5×10^2

from:

$$j_{||\alpha v} = q_\alpha \underbrace{\int\int\int}_{\Gamma(z)} v_{||} f_{\alpha v} d^3v \quad (3)$$

The integration is carried out over the phase space region, $\Gamma(z)$, accessible to the particles at altitude z. Equation (3) gives the current – voltage relationship. The field-aligned current density, $j_{||}(\Delta\Phi, b)$, is a function of $\Delta\Phi{=}\Phi{-}\Phi_m$, the potential difference between altitude z and the magnetospheric end of the flux tube, and $b{=}B/B_m$, the ratio between the local and the magnetospheric magnetic field intensity. Four different populations can be considered:

(A) *The magnetospheric electrons* moving toward the ionosphere are accelerated by a positive potential drop ($\Phi_i{-}\Phi_m{>}0$) along magnetic field lines. The magnetic moment, $\mu{=}m^\alpha v_\perp/\mu_0 B$, as well as the total energy are conserved, thus the longitudinal motion is decelerated by the mirror force of the magnetic field increasing with decreasing altitude. Magnetospheric electrons form the precipitating population that carry energy from the magnetosphere to the ionosphere and also gain energy in the region of the accelerating potential. These particles provide the major contribution to the upward (or direct) current of the auroral circuit. The current density is equal to

$$j^-_{||m} = ebN^-_m \sqrt{\frac{kT^-_m}{2\pi m^-}} \left\{1 - \frac{b-1}{b} e^{-\frac{e(\Phi-\Phi_m)}{(b-1)kT^-_m}}\right\} \quad (4)$$

where N^-_m, T^-_m are the density and temperature of the magnetospheric electrons, e is the elementary charge without algebraic sign, $b{=}B(z)/B_m$ and $\Phi(z)$ depend on the altitude. In this paper, an upward current is considered to be positive.

(B) *The ionospheric electrons* have densities of the order of $10^4\,\mathrm{cm}^{-3}$ at 200 km altitude. Upward moving ionospheric electrons are decelerated by the positive potential drop corresponding to an upward electric field and accelerated by the mirror force. This population contributes to the downward (or return) current. However, their partial current density is very small for positive potential drops greater than 10 Volt. The latter is a threshold determined by the non-linear current-voltage relationship for these species

$$j^-_{||i} = -ebN^-_i \sqrt{\frac{kT^-_i}{2\pi m^-}} e^{-\frac{e(\Phi-\Phi_m)}{kT^-_i}} \left\{1 - \frac{b-1}{b} e^{-\frac{e(\Phi-\Phi_m)}{(b-1)kT^-_i}}\right\} \quad (5)$$

where N^-_i, T^-_i are the density and temperature of the ionospheric electrons. The two partial current densities given in Eqs. (4) and (5) correspond to the current-voltage relationship derived by Knight (1973).

(C) *The upward moving ionospheric ions* are accelerated by both the electrostatic and the mirror force. Thus their upward flux is determined only by their density and temperature at the ionospheric lower boundary of the flux tube. They contribute to the upward leg of the auroral circuit a current density

$$j^+_{||i} = \sum_\alpha |Z^\alpha| eN_{\alpha i} \sqrt{\frac{kT_{\alpha i}}{2\pi m_\alpha}} \quad (6)$$

with a summation over ionospheric positively charged species. Expression (6) is a Jeans flux, derived, for instance, by Lemaire and Scherer (1971) in their exospheric model of the polar wind. In the following we take into account the contributions of H^+, O^+ and He^+. Since the energy of the ionospheric ions is less than 0.1 eV and their density is of the order of $10^4\,\mathrm{cm}^{-3}$, the resulting partial current density is of the order of $10^{-7}\,\mu\mathrm{A/m}^2$, an order of magnitude less than the typical current density of the magnetospheric electrons. A description of the ionospheric parameters used in this study is given in Table 2.

(D) *The magnetospheric ions* are braked both by the mirror force and the positive potential drop between the ionosphere and magnetosphere. Their field-aligned current density is equal to

$$j^+_{||m} = -\sum_\alpha |Z_\alpha| eN_{\alpha m} \sqrt{\frac{kT_{\alpha m}}{2\pi m_\alpha m}} \left(\frac{B_m}{B}\right) e^{-\frac{|Z^\alpha| e(\Phi-\Phi_m)}{kT_{\alpha m}}}. \quad (7)$$

The summation is over all the magnetospheric ion species. Note, however, that for ion densities of the order of $10\,\mathrm{cm}^{-3}$, ion temperatures of the order of 500 eV, and a potential difference between the ionosphere and magnetosphere on the order of 1 kV, the parallel current due to the magnetospheric ions is of the order of $j^+_{||m} \approx 10^{-6}\,(B_m/B_i)$. As we consider a magnetic field ratio less than 10^{-2} the contribution of the magnetospheric ions is negligible and will not be further included in the computations discussed in this paper.

The total, or net, field-aligned current density is then equal to

$$j_{||} = j^-_{||m} + j^-_{||i} + j^+_{||m} + j^+_{||i}. \quad (8)$$

The relationships (4–7) are valid for a positive potential drop, $\Delta\Phi{=}\Phi{-}\Phi_m{>}0$. When $\Delta\Phi$ becomes negative the phase space regions, $\Gamma(z)$, accessible for the populations (A–D) change. Thus the integrals (3) have to be recomputed as shown by Lemaire and Scherer (1971).

The current voltage relationship described by expressions (4–8) is derived assuming that the variation with altitude of the potential is monotonic. A non-monotonic potential variation with the altitude is expected for negative potential drops ($\Phi_i{<}\Phi_m$) since the potential has a minimum where the ambipolar electric field goes to zero (Temerin and Carlson, 1998). The current-voltage relationship for a non-monotonic altitude profile of the potential has been investigated by Temerin and Carlson (1998), Cran-McGreehin and Wright (2005) and Vedin and Rönnmark (2005). In this study, however, we consider only positive potential drops with a monotonic variation with the altitude.

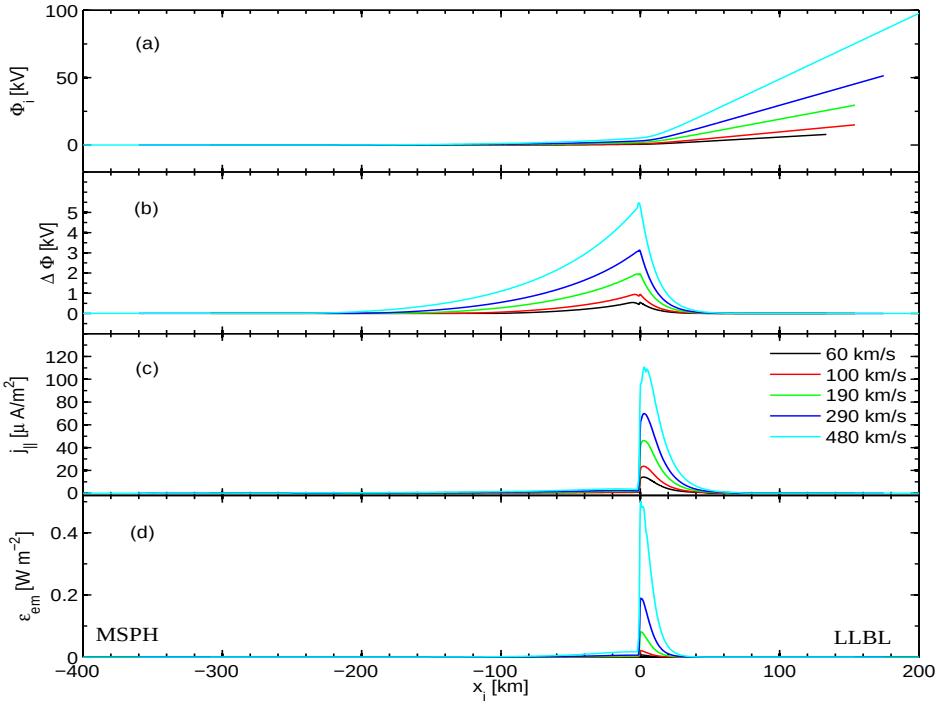

Fig. 4. Solution of Eq. (1) and derived quantities obtained as a function of ionospheric latitude x_i for various bulk velocities on the LLBL side of the TD: **(a)** the ionospheric potential ; **(b)** the field-aligned potential drop; **(c)** the field-aligned current density; **(d)** the flux of precipitating energy. The temperature and density of the magnetospheric and ionospheric populations are given in Tables 1 and 2.

4 Numerical results

In the following we discuss solutions of the current continuity equation obtained for a potential distribution Φ_m, corresponding to a magnetospheric TD.

The solution of the nonlinear equation (1) is integrated numerically in the horizontal direction, over an interval $[x_{i1}, x_{i2}]$. We impose a Dirichlet boundary condition in x_{i1} and x_{i2}, derived from the condition that the net field-aligned current is equal to zero: $j^-_{||m}+j^-_{||i}+j^+_{||i}=0$. In the examples discussed below the boundary value of the potential drop satisfying this condition was in the range of 3–4 Volt. Equation (1) has been discretized using a finite difference method and has been solved numerically with a damped Newton iterative scheme. All the solutions discussed in this paper were obtained for a uniform Pedersen conductivity Σ_P=5 S.

The current continuity equation is evaluated at the ionospheric altitude z_i=200 km. The altitude of the magnetospheric generator is z_m=90 000 km, that is the altitude where, in the conical geometry used for mapping, the intensity of the magnetic field is equal to 30 nT, i.e. the magnetic field intensity used to derive the TD solution. From the condition that the magnetic flux is conserved and assuming a cylindrical mapping (Lyons, 1980), the distance x_m at the magnetospheric altitude z_m, where the magnetic field is B_m, maps at the ionospheric altitude z_i, where the B-field is B_i, according

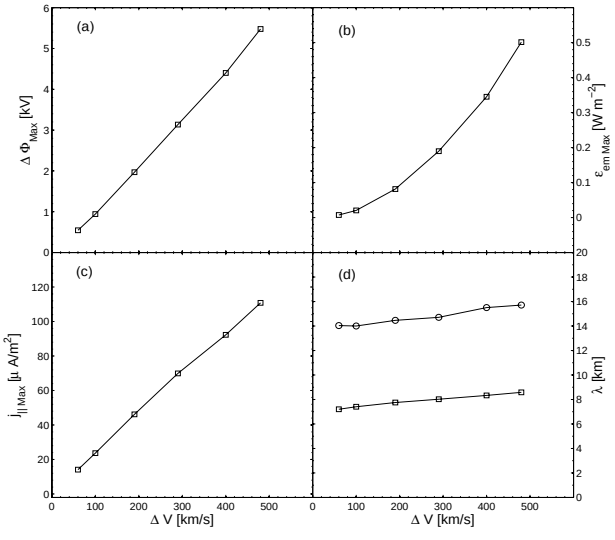

Fig. 5. Variation of arc characteristics as a function of the bulk velocity at the LLBL side of the TD: **(a)** the variation of the maximum of the field-aligned potential drop; **(b)** the variation of the maximum of the flux of precipitating energy; **(c)** the variation of the maximum field-aligned current density; **(d)** the width at half maximum of the current sheet (circles) and of the auroral arc (squares).

to: $x_i = x_m\sqrt{B_m/B_i}$. The current densities at ionospheric altitudes are computed from Eqs. (4–6) by replacing $\Phi=\Phi_i$ and $B=B_i$.

4.1 Effects of the velocity shear

Figure 4 summarizes the results obtained for five different values of the velocity V at the LLBL side, varying from 60 km/s to 480 km/s, thus reflecting different conditions in the solar wind. The region with sheared flow extends over 11 000 km in the transverse direction. It maps into a 600 km interval, x_i=[−400, +200] km, at ionospheric altitudes. The magnetospheric plasma is at rest at the left-hand side of the transition. All the other parameters were kept constant (see Table 1).

The potential distribution obtained from the TD model for various LLBL velocities (illustrated in the first panel of Fig. 2) has been introduced into the expressions (4–7) such that the total field-aligned density can be expressed from Eq. (8) as a function of Φ_m (known) and Φ_i (unknown); $j_{||}$ is then introduced into the current continuity equation (1). The latter is solved for the unknown Φ_i. A first set of solutions is displayed in Fig. 4a. A significant positive field-aligned potential drop between the ionosphere and the magnetosphere, $\Delta\Phi=\Phi_i(x_i)-\Phi(x_m)>0$, is observed in panel (b). It is this positive potential drop that accelerates the magnetospheric electrons. Within a broad ionospheric region, extending over a distance of 200–250 km, the parallel potential drop takes values larger than 100 V. Embedded into the larger structure there is a narrower layer where $\Delta\Phi$ reaches values of the order of several kilovolt, for LLBL velocities larger than 100 km/s.

Figure 4c illustrates the formation of a narrow sheet of upward field-aligned current located at the ionospheric projection of the LLBL segment of the magnetospheric TD. The width of the current sheet is between 10 to 15 km, depending on the velocity shear. The current density is orders of magnitude greater in the ionospheric projection of the LLBL ($x_i>0$) than in the neighboring ionospheric projection of the MSPH region ($x_i<0$).

The luminous intensity of the visible auroral arc is proportional to the incident flux of energy due to precipitating particles, ϵ_{em} (Germany et al., 1997). The latter is illustrated in Fig. 4d. In the broader region associated with potential drops larger than 100 V the flux of precipitating energy takes rather small values. This region could be associated with the faint, diffuse aurora. The region with intense parallel electric field and strong field-aligned currents contains an even narrower region of enhanced flux of precipitating energy that corresponds to an auroral arc. The horizontal distribution of ϵ_{em} suggests that the arc would be brighter (increased precipitating energy) for an increasing shear of the LLBL plasma velocity. The thickness of the visible arc also seems to increase with the velocity shear. Note also that the profile of the precipitating energy, ϵ_{em}, gives information about the perturbation produced by incoming electrons to the ionospheric Pedersen conductivity since $\Sigma_P \propto \sqrt{\epsilon_{em}}$ (Harel et al., 1977; Robinson et al., 1987).

The variation of the arc characteristics with the velocity of the LLBL plasma is summarized in Fig. 5. The peak field-aligned potential drop increases almost linearly with the velocity shear (panel a), as well as the peak of the field-aligned current density (panel c). A nonlinear increase is observed in panel (b) for the maximum of the precipitating energy flux as a function of the the LLBL velocity. This effect is due primarily to an increase of the convection electric field at the LLBL side of the magnetospheric boundary layer. The field-aligned current sheet expands for larger velocities of the LLBL plasma (circles in panel d).

The thickness of the auroral arc is estimated as the width at half maximum of the precipitating energy flux, $\epsilon_{em}(x_i)$. One notes a slight expansion of the arc thickness with increasing LLBL velocity (squares in panel d), in a range of 7 to 9 km. Same panel shows that the field-aligned current sheet is always wider than the arc itself.

4.2 Effects of increasing LLBL density

Figure 6 shows the results obtained for different profiles of the magnetospheric potential, resulting from the TD solutions derived for different values of the LLBL plasma density (see Fig. 3). The TD solution is obtained for the magnetospheric parameters given in Table 1. The general profile of the solution reproduces some of the main characteristics already observed in Figs. 4–5. The field-aligned potential drop tends to decrease with increasing magnetospheric density as shown by Fig. 6b. The field-aligned current density increases with increasing density. A narrow structure in the flux of precipitating energy, which we identify as the auroral arc, is embedded into the larger current sheet (panel d). The precipitating energy flux increases slightly with plasma density at the LLBL side.

The variation of the field-aligned potential drop results mainly from the variation of the ionospheric potential with the LLBL number density (panel a) since the magnetospheric potential is quite insensitive to this change (see top panel of Fig. 3) A more quantitative assessment of the effect of increasing the LLBL density is given in Fig. 7. On one hand, the peak of the field-aligned potential drop decreases with increasing density (panel a). On the other hand, the maximum field-aligned current density increases (panel c) with N_{L}. As the number density of magnetospheric charge carriers has increased there will be a corresponding increment of the current density given by Eq. (4).

Equation (1) shows that an increase of $j_{||}$, the parallel current density, drives a stronger horizontal variation of the ionospheric electric field (i.e., $d^2\Phi_i/dx_i^2$ increases, when Σ_P is constant). Therefore when the LLBL number density increases the ionospheric potential, $\Phi_i(x_i)$, takes values closer to the mapped magnetospheric counterpart, $\Phi_m(x_i)$.

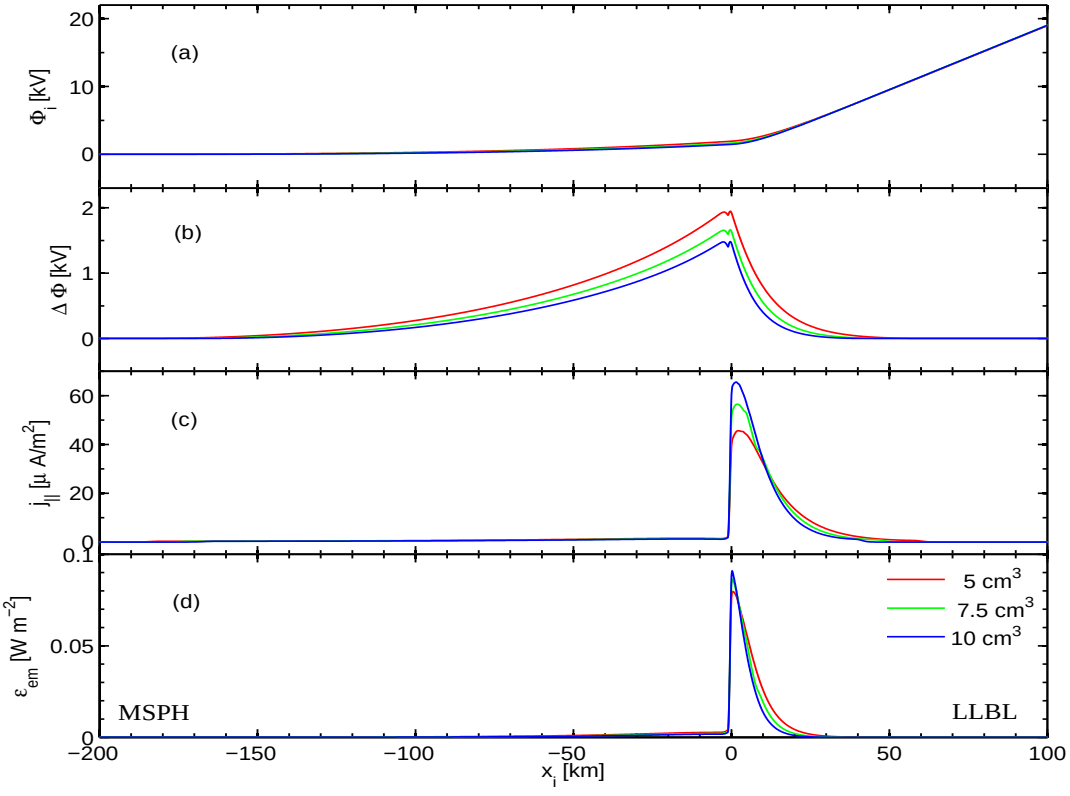

Fig. 6. Solution of Eq. (1) and derived quantities obtained for various densities at the LLBL side of the TD. See caption of Fig. 4. Magnetospheric and ionospheric parameters used to derive these solutions are given in Tables 1 and 2.

Thus the difference between the two, or the field-aligned potential drop, is smaller when the density increases, as shown by Fig. 7a. Not only the potential drop is smaller but it is confined to a narrower region. Consequently the width of the field-aligned current sheet and of the discrete arc decrease when the LLBL density increases as seen in panel (d). A slight increase of the arc luminosity may be associated with an increase of LLBL density, as suggested by panel (b) of Fig. 7.

4.3 Effects of increasing LLBL electron temperature

The effects of an increment of T_L^-, the temperature of the LLBL electrons, have also been investigated. Note that a change of the electron temperature implies a variation of the electron gyroradius. The gyroradius of the LLBL electrons corresponds to the smallest spatial scale intervening in the TD solution. The latter has been recomputed for three different temperatures/gyroradii of the LLBL electrons. As in the previous cases, all the other parameters remain the same (see Table 1) and the LLBL velocity is equal to 190 km/s. The magnetospheric potential profile provided by the TD solution has been again replaced in the current-voltage relationship and the current continuity has been solved. The results are displayed in Figs. 8 and 9.

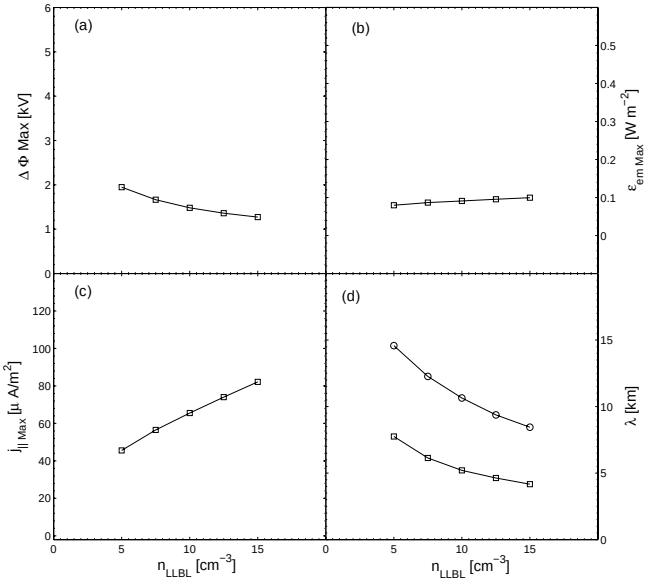

Fig. 7. Variation of arc characteristics as a function of the density at the LLBL side of the TD; same panel description as in the caption of Fig. 5.

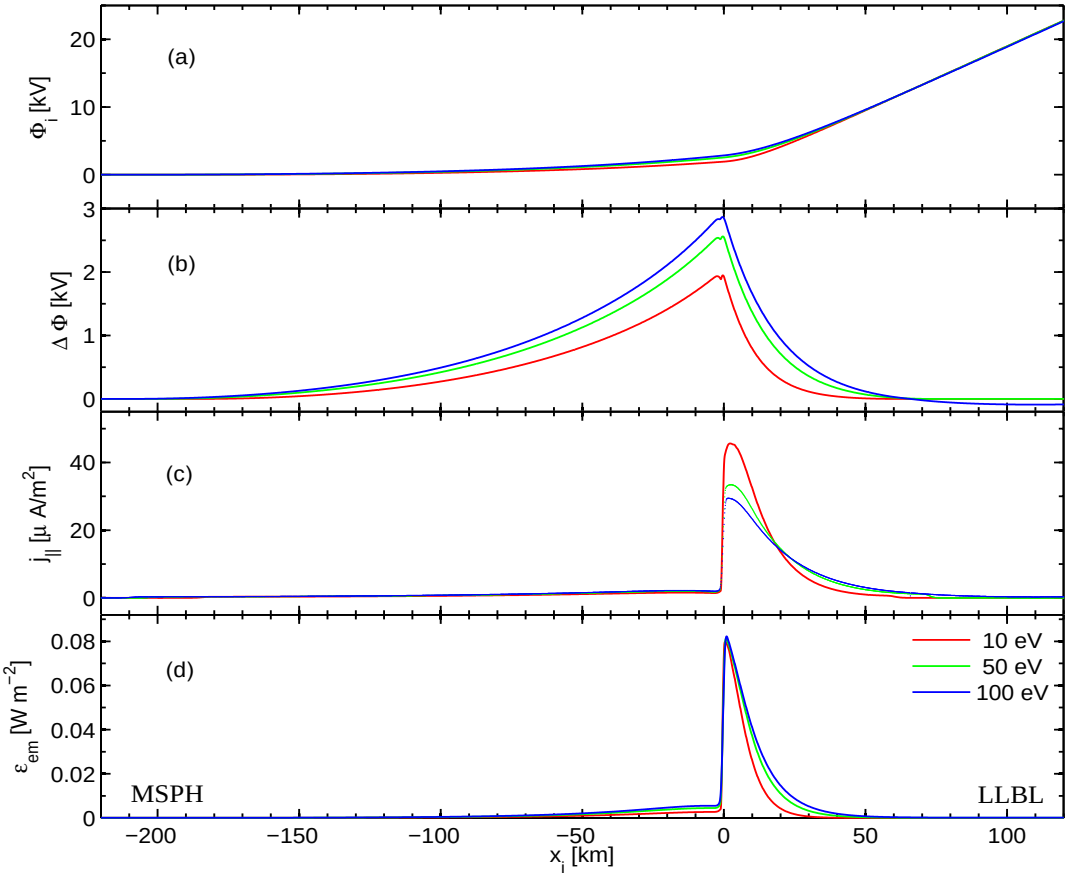

Fig. 8. Solutions of Eq. (1) and derived quantities obtained for various temperatures at the LLBL side of the TD. Magnetospheric and ionospheric parameters are given in Tables 1 and 2; same panel format as in Fig. 4.

The flux of precipitating energy remains roughly constant for an increase of T_{L}^{-} of one order of magnitude (see Figs. 8d and 9b). Thus the intensity of the auroral arc remains virtually unchanged when the electron temperature of the magnetospheric moving plasma increases.

The current density however diminishes (Figs. 8c and 9c). This can be understood by inspecting Eq. (4) where one notes that the nonlinear term is dominant. Therefore an increase of the LLBL electron temperature indeed implies a reduction of the corresponding field-aligned current density. One also notes from the current continuity equation that the reduction of the parallel current density implies that the ionospheric electric field has a smoother variation with x_i (smaller "curvature", $d^2\Phi_i/dx_i^2$, of the potential profile). Thus the higher T_{L}^{-}, the larger is the difference between $\Phi_i(x_i)$ and $\Phi_m(x_i)$, i.e. the larger is the field-aligned potential drop. An increment of $\Delta\Phi$ with increasing T_{L}^{-} is indeed observed in Figs. 8b and 9a.

The region with a significant field-aligned potential drop is broader for larger LLBL electron temperature (Fig. 8b). On one hand this is a consequence of a smaller $j_{||}$ as explained above. On the other hand, the width of the generator TD is larger when T_{L}^{-} increases. The spatial scale of the TD is determined by the magnetospheric VDF through the parameters $l_{M,L}^{+/-}$ (see Appendix A) and the Larmor radii. An increase of the electron Larmor radius produces a broader transition layer. The increment of the width of both the parallel current sheet and the auroral arc is observed in Fig. 9d. The arc width stays under a threshold of 10 km, while the width of the field-aligned current sheet increases up to 20 km as Fig. 9 shows.

5 Summary and conclusions

We have shown that magnetospheric sheared flows confined in a transition layer at the LLBL/MSPH interface can act as a generator identified with the electromotive force required for the auroral current circuit. The source of energy is the external driver that sustains the flow and the gradients of velocity, density and/or temperature. If this driver is able to maintain such gradients over time intervals longer than the Alfven travel time between the magnetosphere and ionosphere, one

can find a quasi-static solution. In this case, kinetic solutions for sheared flows in the generator can be found for transitions of tangential discontinuity type. These solutions provide the electrostatic field and all moments of the VDF (in particular number and current density), given the asymptotic conditions for the plasma state and for the fields.

The parallel flux of charged particles emerging both from the magnetospheric generator and the ionosphere can be computed analytically as functions of the potential difference between the generator and the load (the ionosphere). The fundamental equation that couples the "field-aligned" and "horizontal" quantities is the current continuity equation at the top of the ionosphere. Numerical solutions of this equation have been found by imposing the boundary condition that the total parallel current is equal to zero at the left and right-hand sides of the integration domain.

We were able to investigate the "natural" scaling of the auroral structure, determined by the characteristics of the TD generator, the current-voltage relationship, the characteristics of the magnetospheric and ionospheric populations and the mapping between the two ends of the flux tube. In this work we have developed a parameter study in which we have investigated the effects on the intensity and scale of the auroral structures of magnetospheric parameters like the velocity shear, density and temperature. In all the computations discussed in this paper the Pedersen conductivity was assumed uniform and constant. In reality the conductivity may be non-uniform. Furthermore, the flux of precipitating electrons may produce excess ionization, thus increasing Σ_P and generating a feed-back on the overall circuit balance. As argued by Roth et al. (1993), in a steady-state situation that implies a zero circulation of the E-field along the auroral circuit, an increase of Σ_P will diminish the ionospheric potential differences but will enhance the field-aligned ones. Thus we conjecture that the ionospheric feed-back will enhance the ionospheric effects obtained with our steady-state model.

A positive potential drop with a peak of the order of several kilovolt has been found in almost all the cases discussed in this study. The maximum potential drop ranges from 700 and 5500 V when the LLBL velocity varies from 60 to 480 km/s. The region of field-aligned potential drop expands when the LLBL plasma velocity increases. However, only within a narrower region the potential drop takes values exceeding 1 kV. Significant field-aligned currents flow out of the ionosphere in a much narrower sheet. The width of the field-aligned current sheet ranges from 14 to 20 km at 200 km altitude. The current density increases with increasing LLBL plasma velocity and density. It decreases when the LLBL plasma temperature increases. The spatial characteristics of the magnetospheric TD determine the overall behavior of the ionospheric current density. The jump in the parallel current density out of the ionosphere (panels c in Figs. 4, 6 and 8) coincides with the mapped position of the jump observed in the magnetospheric plasma density (middle panels in Figs. 2 and 3).

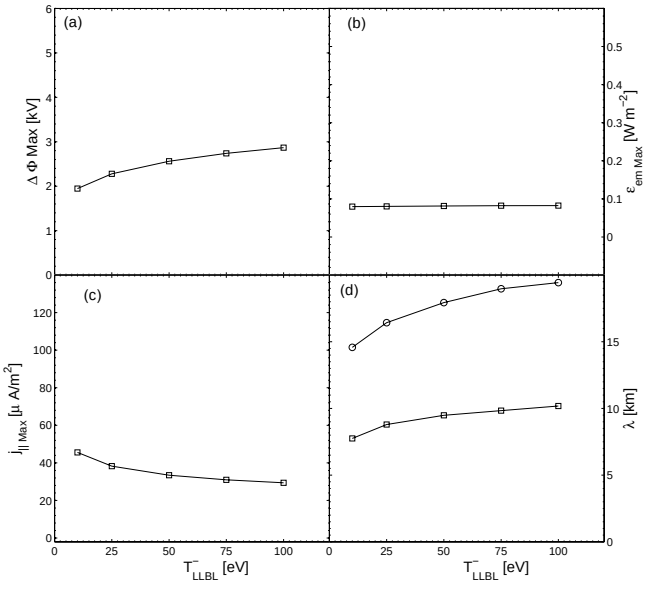

Fig. 9. Variation of arc characteristics as a function of the temperature at the LLBL side of the TD. See caption of Fig. 5 for a description of panels.

The contribution of the ionospheric species to the field-aligned current density is rather small in the cases investigated in this study, except for the boundary regions. It is the contribution close to the edges of the integration domain that enabled us to satisfy the imposed boundary conditions and to obtain convergent solutions using the exact expressions of the current-voltage relationship and not linearized ones as in previous studies (Lyons, 1980, 1981).

The region where the energy precipitation reaches significant values is the narrowest structure observed in the solution. It would correspond to a discrete auroral arc. In our solutions the thickness of the arc takes typical values in the range of 5 to 10 km, depending on the parameters of the LLBL/MSPH transition layer. It corresponds to typical discrete auroral arcs of the order of 1–10 km in latitudinal extent that dominate in visible spectrum (Evans, 1974; Knudsen et al., 2001). We have also shown that the arc tends to be brighter and wider when the convection in the LLBL is faster, i.e. for rapid solar wind. The model predicts that the arc tends to become thinner and more intense when the density of the LLBL plasma increases (and the LLBL velocity remains unchanged). Finally, our results suggest that the arc keeps the same luminosity but expands in width when the LLBL temperature increases while the LLBL density and velocity remain unchanged.

This study demonstrates that sheared plasma flows in outer layers of the magnetosphere, driven by the interaction with a variable solar wind, can provide the required energy for the activation of discrete auroral arcs. It also shows how the intensity and scale of the ionospheric phenomena vary with the

plasma parameters at the magnetospheric shear flow interface. The model contributes to the quantitative description of the quasi-static coupling of the magnetosphere with the polar ionosphere and provides interesting opportunities for verification by in-situ and ground based data.

Appendix A

In Sect. 2 we have briefly discussed the kinetic model of a tangential discontinuity applied to a one-dimensional boundary layer interfacing sheared plasma flows. Here we give the expressions for the velocity distribution function (VDF) of each constituent as well as for some of its moments: the number and current density. These results are obtained from the general formulation of the kinetic TD model of Roth et al. (1996).

The plasma interface is considered as a planar plasma transition layer of finite thickness. When $x_m \to \mp\infty$ it is assumed that the plasma, composed of protons and electrons, is described by a displaced Maxwellian velocity distribution functions. At any point inside the transition layer the velocity distribution functions correspond to the interpenetration of these two hydrogen plasmas in the form given in Roth et al. (1996). The plasma boundary conditions describe, on the left-hand side ($x_m \to -\infty$), the magnetospheric plasma (subscript M) with uniform number densities ($N_{\rm M}^- = N_{\rm M}^+ = N_{\rm M}$) and temperatures ($T_{\rm M}^-$, $T_{\rm M}^+$), and on the right-hand side ($x_m \to +\infty$), the LLBL plasma (subscript L) with uniform number densities ($N_{\rm L}^- = N_{\rm L}^+ = N_{\rm L}$) and temperatures ($T_{\rm L}^-$, $T_{\rm L}^+$).

The magnetic field direction is everywhere parallel to the z-axis. This implies that the vector potential is directed along the y-axis ($\mathbf{A} = a\mathbf{e}_y$). For both plasma populations (MSPH and LLBL) the partial electric current densities of protons (+) and electrons (−) are parallel to the y-axis ($\mathbf{j}_{\rm M}^{+,-} = j_{\rm M}^{+,-}\mathbf{e}_y$, $\mathbf{j}_{\rm L}^{+,-} = j_{\rm L}^{+,-}\mathbf{e}_y$). The electric field is in the x_m-direction ($\mathbf{E} = E_x\mathbf{e}_x$). The plasma flow ($\mathbf{V}$) is parallel to the y-axis and is equal respectively to $V_{\rm M}$ on MSPH side (where $x_m \to -\infty$) and $V_{\rm L}$ on LLBL side (where $x_m \to +\infty$). Note that in all the cases discussed in this study the plasma velocity at the left-hand side vanishes, $V_{\rm M} = 0$.

The solution of the Vlasov equation for each constituent α is a combination between $F_{\rm M}^\alpha(m_\alpha, N_{\rm M}^\alpha, T_{\rm M}^\alpha, V_{M,y}, l_M^\alpha)$ describing the plasma at the left (magnetospheric) side and $F_{\rm L}^\alpha(m_\alpha, N_{\rm L}^\alpha, T_{\rm L}^\alpha, V_{L,y}, l_{\rm L}^\alpha)$ at the right (LLBL) side. The velocity distribution function may be then written as a function of the constants of motion (H and p_y, see Sect. 2.1) as below:

$$F^\alpha = c_{\rm M}^\alpha e^{-\left[\frac{H}{kT_{\rm M}^\alpha} + \frac{m_\alpha V_{\rm M}^2}{2kT_{\rm M}^\alpha} - \frac{p_y V_{\rm M}}{kT_{\rm M}^\alpha}\right]} \mathrm{erfc}(U_{\rm M}^\alpha) + c_L^\alpha e^{-\left[\frac{H}{kT_{\rm L}^\alpha} + \frac{m_\alpha V_{\rm L}^2}{2kT_{\rm L}^\alpha} - \frac{p_y V_{\rm L}}{kT_{\rm L}^\alpha}\right]} \mathrm{erfc}(-U_{\rm L}^\alpha) \quad \text{(A1)}$$

where we defined:

$$c_{\rm M}^\alpha = \frac{N_{\rm M}^\alpha}{2}\left(\frac{m_\alpha}{2\pi k T_{\rm M}^\alpha}\right)^{3/2} \qquad c_L^\alpha = \frac{N_{\rm L}^\alpha}{2}\left(\frac{m_\alpha}{2\pi k T_{\rm L}^\alpha}\right)^{3/2}$$

The functions $U_{\rm M}^\alpha$ and $U_{\rm L}^\alpha$ depend on the canonical momentum component p_y:

$$U_{\rm M}^\alpha = \frac{p_y - m_\alpha V_{\rm M}^\alpha}{Z^\alpha e B_{\rm M} \rho_{\rm M}^\alpha \sqrt{(l_{\rm M}^\alpha)^2 - 1}}$$

$$U_{\rm L}^\alpha = \frac{p_y - m_\alpha V_{\rm L}^\alpha}{Z^\alpha e B_{\rm L} \rho_{\rm L}^\alpha \sqrt{(l_{\rm L}^\alpha)^2 - 1}}$$

where $\rho_{\rm M}^\alpha$, $\rho_{\rm L}^\alpha$ are the Larmor radius at the two sides of the discontinuity:

$$\rho_{\rm M}^\alpha = \frac{\sqrt{2m_\alpha k T_{\rm M}^\alpha}}{|Z^\alpha| e B_{\rm M}} \qquad \rho_{\rm L}^\alpha = \frac{\sqrt{2m_\alpha k T_{\rm L}^\alpha}}{|Z^\alpha| e B_{\rm L}}$$

In the above notations α stands for the species (− for electrons and + for protons). The parameters $l_{\rm M}^\alpha$ and $l_{\rm L}^\alpha$ were introduced to control the thickness of the TD. The values of $l_{\rm M}^\alpha$ and $l_{\rm L}^\alpha$ used to obtained the solutions shown in Figs. 2–3 are given in Table 1.

The partial number densities $n^- = n_{\rm M}^- + n_{\rm L}^-$; $n^+ = n_{\rm M}^+ + n_{\rm L}^+$ and the partial current densities $j_y^- = j_M^- + j_L^-$; $j_y^+ = j_M^+ + j_L^+$, are analytical functions of Φ_m and a obtained as moments of the VDF given in Eq. (A1). The partial number densities are given by:

$$n_{\rm M}^- = \frac{N_{\rm M}}{2} e^{+\frac{e(\Phi_m - aV_{\rm M})}{kT_M^-}} \mathrm{erfc}\left(+\frac{a}{l_{\rm M}^- \rho_M^- B_M}\right) \quad \text{(A2)}$$

$$n_{\rm M}^+ = \frac{N_{\rm M}}{2} e^{-\frac{e(\Phi_m - aV_{\rm M})}{kT_M^+}} \mathrm{erfc}\left(+\frac{a}{l_{\rm M}^+ \rho_M^+ B_M}\right) \quad \text{(A3)}$$

$$n_{\rm L}^- = \frac{N_{\rm L}}{2} e^{+\frac{e(\Phi_m - aV_{\rm L})}{kT_L^-}} \mathrm{erfc}\left(-\frac{a}{l_{\rm L}^- \rho_L^- B_L}\right) \quad \text{(A4)}$$

$$n_{\rm L}^+ = \frac{N_{\rm L}}{2} e^{-\frac{e(\Phi_m - aV_{\rm L})}{kT_L^+}} \mathrm{erfc}\left(-\frac{a}{l_{\rm L}^+ \rho_L^+ B_L}\right) \quad \text{(A5)}$$

The partial current densities are equal to:

$$j_M^- = -J_M^- G_M^- - e n_M^- V_{\rm M} \quad \text{(A6)}$$

$$j_M^+ = -J_M^+ G_M^+ + e n_M^+ V_{\rm M} \quad \text{(A7)}$$

$$j_L^- = J_L^- G_L^- - e n_L^- V_{\rm L} \quad \text{(A8)}$$

$$j_L^+ = J_L^+ G_L^+ + e n_L^+ V_{\rm L} \quad \text{(A9)}$$

where the functions J and G are defined as:

$$J_\nu^\alpha = \frac{|Z^\alpha| e N_\nu^\alpha}{l_\nu^\alpha}\left(\frac{kT_\nu^\alpha}{2\pi m_\alpha}\right)^{1/2} \quad \text{(A10)}$$

$$G_\nu^\alpha = \exp\left\{-\left[\frac{Z^\alpha e(\Phi_m - aV_\nu)}{kT_\nu^\alpha} + \left(\frac{a}{l_\nu^\alpha \rho_\nu^\alpha B_\nu}\right)^2\right]\right\} \quad \text{(A11)}$$

with ν an index corresponding to the origin of the population (M for left-hand side or magnetospheric and L for right-hand side or LLBL). In Eqs. (A2) through (A9) erfc is the complementary error function, e is the magnitude of elementary charge, k is the Boltzmann constant, B_{M} and B_{L} are respectively the magnitude of the magnetic field deep at the left hand side (at large negative values of x_m) and at right hand side (at large positive values of x). The parameters l_{M}^{-}, l_{M}^{+}, l_{L}^{-} and l_{L}^{+} measure the "thickness" of the four transitions that the different particle populations undergo taking as thickness unit the asymptotic thermal Larmor gyroradii, $\rho_{M,L}^{-}$ and $\rho_{M,L}^{+}$. Their exact values are chosen on the basis of both theoretical and observational facts. It is clear that the transition thickness is expected to be scaled according to some small microscopic parameter. In magnetized collisionless plasmas this small parameter is the particle Larmor radius, at least when the plasma is quasi-neutral.

Acknowledgements. M. Echim is beneficiary of a fellowship granted by the Belgian Federal Science Policy Office (Project MO/35/016, "Electrodynamic coupling of the auroral ionosphere and magnetosphere").

Topical Editor I. A. Daglis thanks I. Voronkov and another referee for their help in evaluating this paper.

References

Angelopoulos, V., Baumjohann, W., Kennel, C. F., Coroniti, F. V., Kivelson, M. G., Pellat, R., Walker, R. J., Luehr, H., and Paschmann, G.: Bursty bulk flows in the inner central plasma sheet, J. Geophys. Res., 97, 4027–4039, 1992.

Baumjohann, W. G., Paschmann, G., and Luehr, H.: Characteristics of high-speed ion flows in the plasma sheet, J. Geophys. Res., 95, 3801–3809, 1990.

Cao, J. B., Ma, Y. D., Parks, G., Rème, H., Dandouras, I., Nakamura, R., Zhang, T. L., Zong, Q., Lucek, E., Carr, C. M., Liu, Z. X., and Joint, G. C.: Observations by Cluster satellites of bursty bulk flows in the magnetotail, J. Geophys. Res., 111, A04206, doi:10.1029/2005JA011322, 2006.

Cran-McGreehin, A. and Wright, A.: Current-voltage relationship in downward field-aligned current region, J. Geophys. Res., 110, A10S10, doi:10.1029/2004JA010870, 2005.

De Keyser, J. and Roth, M.: Equilibrium conditions for the tangential discontinuity magnetopause, J. Geophys. Res., 102, 9513–9530, 1997a.

De Keyser, J. and Roth, M.: Equilibrium conditions for the tangential discontinuity magnetopause (correction), J. Geophys. Res., 102, 19 943–19 944, 1997b.

De Keyser, J.: Formation and evolution of subauroral ion drifts in the course of a substorm, J. Geophys. Res., 104(6), 12 339–12 350, 1999.

Echim, M. and Lemaire, J.: Two-dimensional solution for a collisionless plasma jet across transverse magnetic field lines with a sheared bulk velocity, Phys. Rev. E, 72, 036405, doi:10.1103/PhysRevE.72.036905, 2005.

Evans, D. S.: Precipitating electron fluxes formed by a magnetic field-aligned potential difference, J. Geophys. Res., 79, 2853–2858, 1974.

Fairfield, D.H ., Mukai, T., Brittnacher, M., Reeves, G. D., Kokubun, S., Parks, G. K., Nagai, T., Matsumoto, H., Hashimoto, K., Gurnett, D. A., and Yamamoto, T.: Earthward flow bursts in the inner magnetotail and their relation to auroral brightenings, AKR intensification, geosynchronous particle injections and magnetic activity, J. Geophys. Res., 104, 355–370, 1999.

Fridman, M. and Lemaire, J.: Relationship between auroral electron fluxes and field-aligned electric potential differences, J. Geophys. Res., 85, 664–670, 1980.

Germany, G. A., Parks, G. K., Brittnacher, M., Cumnock, J., Lummerzheim, D., Spann, J. F., Chen, L., Richards, P. G., and Rich, F. J.: Remote determination of auroral energy characteristics during substorm activity, Geophys. Res. Lett., 24(8), 995–998, 1997.

Grigorenko, E. E., Fedorov, A., and Zelenyi, L. M.: Statistical study of transient plasma structures in magnetotail lobes and plasma sheet boundary layer: Interball-1 observations, Ann. Geophys., 20, 329–340, 2002, http://www.ann-geophys.net/20/329/2002/.

Harel, M., Wolf, R. A., Reiff, P. H., and Hillis, H. K.: Study of plasma flow near the Earth's plasmapause, Rep. AFGL-TR-77-286, U.S. Air Force Geophys. Lab, Hanscom, AFB, Mass., 1977.

Knight, S.: Parallel electric fields, Planet. Space Sci., 21, 741–750, 1973.

Knudsen, D. J., Donovan, E. F., Cogger L. L., Jackel, B., and Shaw, W. D.: Width and structure of mesoscale optical auroral arcs, Geophys. Res. Lett. 28(4), 705–708, 2001.

Lemaire, J. and Scherer, M.: Simple model for an ion-exosphere in an open magnetic field, Phys. Fluids, 14, 1683–1694, 1971.

Lemaire, J. and Scherer, M.: Plasma sheet particle precipitation: A kinetic model, Planet. Space Sci., 21, 281–289, 1973.

Lundin, R. and Evans, D.: Boundary layer plasmas as a source for high-latitude, early afternoon, auroral arcs, Planet. Space Sci., 33(12), 1389–1406, 1985.

Lyons, L. R.: Generation of large-scale regions of auroral currents, electric potentials and precipitation by the divergence of the convection electric field, J. Geophys. Res., 85, 17–24, 1980.

Lyons, L. R.: Discrete aurora a the direct result of an inferred high altitude generating potential distribution, J. Geophys. Res., 86, 1–8, 1981.

Nakamura, R., Baumjohann, W., Schodel, R., Brittnacher, M., Sergeev, V. A., Kubyshkina, M., Mukai, T., and Liou, K.: Earthward flow bursts, auroral streamers, and small expansions J. Geophys. Res., 106(A6), 10 791–10 802, 2001.

Phan, T. D., Larson, D., McFadden, J., Lin, R. P., Carlson, C., Moyer, M., Paularena, K. I., McCarthy, M., Parks, G. K., Rème, H., Sanderson, T. R., and Lepping, R. P.: Low-latitude dusk flank magnetosheath, magnetopause, and boundary layer for low magnetic shear: Wind observations, J. Geophys. Res., 102(A9), 19 883–19 896, 1997.

Pierrard, V.: New model of magnetospheric current-voltage relationship J. Geophys. Res., 101, 2669–2676, 1996.

Robinson, R., Vondrak, R., Miller, K., Dabbs, T., and Hardy, D.: On calculating ionospheric conductances from the flux and energy of precipitating electrons, J. Geophys. Res., 92, 2565–2569, 1987.

Roth, M., Evans, D., and Lemaire, J.: Theoretical structure of a magnetospheric plasma boundary: application to the formation of discrete auroral arcs, J. Geophys. Res., 98, 11 411–11 423, 1993.

Roth, M., De Keyser, J., and Kuznetsova, M. M.: Vlasov theory of the equilibrium structure of tangential discontinuities in space plasmas, Space Sci. Rev., 76, 251–317, 1996.

Sergeev, V. A., Liou, K., Meng, C.-I., Newell, P. T., Brittnacher, M., Parks, G., and Reeves, G. D.: Development of auroral streamers in association with localized impulsive injections to the inner magnetotail, Geophys. Res. Lett., 26, 417–420, 1999.

Temerin, M. and Carlson, C. W.: Current-voltage relationship in the downward auroral current region, Geophys. Res. Lett., 25(13), 2365–2368, 1998.

Vaisberg, O. L., Smirnov, V. N., Avanov, L. A., Waite Jr., J. H., Burch, J. L., Gallagher, D. L., and Borodkova, N. L.: Different types of low-latitude boundary layer as observed by Interball Tail probe, J. Geophys. Res., 106, 13 067–13 090, 2001.

Vedin, J. and Rönnmark, K.: Electrostatic potentials in the downward auroral current region, J. Geophys. Res., 110, A08207, doi:10.1029/2005JA011083, 2005.

Zesta, E., Lyons, L., and Donovan, E.: The auroral signature of Earthward flow bursts observed in the magnetotail, Geophys. Res. Lett., 27, 3241–3244, 2000.

Whipple Jr., E. C.: The signature of parallel electric fields in a collisionless plasma, J. Geophys. Res., 82, 1525–1531, 1977.